

# Initial Measurements of Z-Boson Resonance Parameters in $e^+e^-$ Annihilation

G. S. Abrams,<sup>(1)</sup> C. E. Adolphsen,<sup>(2)</sup> R. Aleksan,<sup>(3)</sup> J. P. Alexander,<sup>(3)</sup> M. A. Allen,<sup>(3)</sup> W. B. Atwood,<sup>(3)</sup> D. Averill,<sup>(4)</sup> J. Ballam,<sup>(3)</sup> P. Bambade,<sup>(3)</sup> B. C. Barish,<sup>(5)</sup> T. Barklow,<sup>(3)</sup> B. A. Barnett,<sup>(6)</sup> J. Bartelt,<sup>(3)</sup> S. Bethke,<sup>(1)</sup> D. Blockus,<sup>(4)</sup> W. de Boer,<sup>(3)</sup> G. Bonvicini,<sup>(7)</sup> A. Boyarski,<sup>(3)</sup> B. Brabson,<sup>(4)</sup> A. Breakstone,<sup>(8)</sup> M. Breidenbach,<sup>(3)</sup> J. M. Brom,<sup>(4)</sup> J. L. Brown,<sup>(3)</sup> K. L. Brown,<sup>(3)</sup> F. Bulos,<sup>(3)</sup> P. R. Burchat,<sup>(2)</sup> D. L. Burke,<sup>(3)</sup> R. J. Cence,<sup>(8)</sup> J. Chapman,<sup>(7)</sup> M. Chmeissani,<sup>(7)</sup> J. Clendenin,<sup>(3)</sup> D. Cords,<sup>(3)</sup> D. P. Coupal,<sup>(3)</sup> P. Dauncey,<sup>(6)</sup> N. R. Dean,<sup>(3)</sup> H. C. DeStaebler,<sup>(3)</sup> D. E. Dorfan,<sup>(2)</sup> J. M. Dorfan,<sup>(3)</sup> P. S. Drell,<sup>(1)</sup> D. C. Dreuer,<sup>(6)</sup> F. Dydak,<sup>(3)</sup> S. Ecklund,<sup>(3)</sup> R. Elia,<sup>(3)</sup> R. A. Erickson,<sup>(3)</sup> J. Fay,<sup>(1)</sup> G. J. Feldman,<sup>(3)</sup> D. Fernandes,<sup>(3)</sup> R. C. Field,<sup>(3)</sup> T. H. Fieguth,<sup>(3)</sup> G. E. Fischer,<sup>(3)</sup> W. T. Ford,<sup>(9)</sup> C. Fordham,<sup>(3)</sup> R. Frey,<sup>(7)</sup> D. Fujino,<sup>(3)</sup> K. K. Gan,<sup>(3)</sup> C. Gatto,<sup>(2)</sup> E. Gero,<sup>(7)</sup> G. Gidal,<sup>(1)</sup> T. Glanzman,<sup>(3)</sup> G. Goldhaber,<sup>(1)</sup> J. J. Gomez Cadenas,<sup>(2)</sup> G. Gratta,<sup>(2)</sup> G. Grindhammer,<sup>(3)</sup> P. Grosse-Wiesmann,<sup>(3)</sup> G. Hanson,<sup>(3)</sup> R. Harr,<sup>(1)</sup> B. Harral,<sup>(6)</sup> F. A. Harris,<sup>(8)</sup> C. M. Hawkes,<sup>(5)</sup> K. Hayes,<sup>(3)</sup> C. Hearty,<sup>(1)</sup> D. Herrup,<sup>(1)</sup> C. A. Heusch,<sup>(2)</sup> M. D. Hildreth,<sup>(3)</sup> T. Himel,<sup>(3)</sup> D. A. Hinshaw,<sup>(9)</sup> S.-O. Holmgren,<sup>(1)</sup> S. J. Hong,<sup>(7)</sup> D. Hutchinson,<sup>(3)</sup> A. Hutton,<sup>(3)</sup> J. Hylen,<sup>(6)</sup> W. R. Innes,<sup>(3)</sup> R. G. Jacobsen,<sup>(3)</sup> M. Jaffre,<sup>(1)</sup> J. A. Jaros,<sup>(3)</sup> R. K. Jobe,<sup>(3)</sup> C. K. Jung,<sup>(3)</sup> J. A. Kadyk,<sup>(1)</sup> D. Karlen,<sup>(3)</sup> J. Kent,<sup>(2)</sup> M. King,<sup>(2)</sup> S. R. Klein,<sup>(3)</sup> D. S. Koetke,<sup>(3)</sup> S. Komamiya,<sup>(3)</sup> W. Koska,<sup>(7)</sup> L. A. Kowalski,<sup>(3)</sup> W. Kozanecki,<sup>(3)</sup> J. F. Kral,<sup>(1)</sup> M. Kuhlen,<sup>(5)</sup> A. V. Kulikov,<sup>(3)</sup> L. Labarga,<sup>(2)</sup> A. J. Lankford,<sup>(3)</sup> R. R. Larsen,<sup>(3)</sup> F. Le Diberder,<sup>(3)</sup> M. E. Levi,<sup>(1)</sup> A. M. Litke,<sup>(2)</sup> T. Lohse,<sup>(3)</sup> V. Lüth,<sup>(3)</sup> G. R. Lynch,<sup>(1)</sup> J. A. McKenna,<sup>(5)</sup> J. A. J. Matthews,<sup>(6)</sup> T. Mattison,<sup>(3)</sup> B. D. Milliken,<sup>(5)</sup> K. C. Moffeit,<sup>(3)</sup> C. T. Munger,<sup>(3)</sup> J. J. Murray,<sup>(3)</sup> W. N. Murray,<sup>(4)</sup> J. Nash,<sup>(3)</sup> H. Ogren,<sup>(4)</sup> R. A. Ong,<sup>(3)</sup> K. F. O'Shaughnessy,<sup>(3)</sup> S. I. Parker,<sup>(8)</sup> C. Peck,<sup>(5)</sup> M. L. Perl,<sup>(3)</sup> F. Perrier,<sup>(3)</sup> A. Petersen,<sup>(3)</sup> M. Petradza,<sup>(7)</sup> N. Phinney,<sup>(3)</sup> R. Pitthan,<sup>(3)</sup> F. C. Porter,<sup>(5)</sup> P. Rankin,<sup>(9)</sup> J. R. Rees,<sup>(3)</sup> J. D. Richman,<sup>(1)</sup> K. Riles,<sup>(3)</sup> L. Rivkin,<sup>(3)</sup> M. C. Ross,<sup>(3)</sup> F. R. Rouse,<sup>(3)</sup> D. R. Rust,<sup>(4)</sup> H. F. W. Sadrozinski,<sup>(2)</sup> M. W. Schaad,<sup>(1)</sup> T. L. Schalk,<sup>(9)</sup> B. A. Schumm,<sup>(1)</sup> A. S. Schwarz,<sup>(2)</sup> J. T. Seeman,<sup>(3)</sup> A. Seiden,<sup>(2)</sup> J. C. Sheppard,<sup>(3)</sup> J. G. Smith,<sup>(3)</sup> A. Snyder,<sup>(4)</sup> E. Soderstrom,<sup>(5)</sup> R. Stiening,<sup>(3)</sup> D. P. Stoker,<sup>(6)</sup> R. Stroynowski,<sup>(5)</sup> M. Swartz,<sup>(3)</sup> R. Thun,<sup>(7)</sup> N. Toge,<sup>(3)</sup> G. H. Trilling,<sup>(1)</sup> R. Van Kooten,<sup>(3)</sup> P. Voruganti,<sup>(3)</sup> S. R. Wagner,<sup>(9)</sup> S. Watson,<sup>(2)</sup> P. Weber,<sup>(9)</sup> A. Weigend,<sup>(3)</sup> A. J. Weinstein,<sup>(5)</sup> A. J. Weir,<sup>(5)</sup> S. L. White,<sup>(9)</sup> E. Wicklund,<sup>(5)</sup> R. C. Wolf,<sup>(5)</sup> D. R. Wood,<sup>(1)</sup> M. Woods,<sup>(3)</sup> G. Wormser,<sup>(3)</sup> R. Wright,<sup>(3)</sup> D. Y. Wu,<sup>(5)</sup> M. Yurko,<sup>(4)</sup> C. Zaccardelli,<sup>(2)</sup> and C. von Zanthier<sup>(2)</sup>

<sup>(1)</sup>Lawrence Berkeley Laboratory and Department of Physics, University of California, Berkeley, California 94720

<sup>(2)</sup>University of California, Santa Cruz, California 95064

<sup>(3)</sup>Stanford Linear Accelerator Center, Stanford University, Stanford, California 94309

<sup>(4)</sup>Indiana University, Bloomington, Indiana 47405

<sup>(5)</sup>California Institute of Technology, Pasadena, California 91125

<sup>(6)</sup>Johns Hopkins University, Baltimore, Maryland 21218

<sup>(7)</sup>University of Michigan, Ann Arbor, Michigan 48109

<sup>(8)</sup>University of Hawaii, Honolulu, Hawaii 96822

<sup>(9)</sup>University of Colorado, Boulder, Colorado 80309

(Received 24 July 1989)

We have measured the mass of the Z boson to be  $91.11 \pm 0.23 \text{ GeV}/c^2$ , and its width to be  $1.61 \pm 0.49 \text{ GeV}$ . If we constrain the visible width to its standard-model value, we find the partial width to invisible decay modes to be  $0.62 \pm 0.23 \text{ GeV}$ , corresponding to  $3.8 \pm 1.4$  neutrino species.

PACS numbers: 14.80.Er, 13.38.+c, 13.65.+i

We present measurements by the Mark II detector at the SLAC Linear Collider (SLC) of the  $e^+e^-$  annihilation cross section over a range of center-of-mass energies ( $E$ ) from 89.2 to 93.0 GeV, in which the annihilation process is dominated by the resonant formation of the Z boson and its subsequent decay. A total of  $5.8 \pm 0.5 \text{ nb}^{-1}$  of data have been recorded at six energy settings separated by approximately 0.75 GeV. We have determined values of the Z mass and width from these measurements. The mass ( $m_Z$ ) can be interpreted as one of three fundamental parameters describing the elec-

troweak interactions, the others being the fine-structure constant and the Fermi constant. The width measures the coupling of the Z to all fundamental particles with mass less than  $m_Z/2$ .

The SLC is the first operating single-pass electron-positron collider.<sup>1</sup> An electron bunch and a positron bunch, each containing of order  $10^{10}$  particles, are accelerated simultaneously in the SLAC linear accelerator, magnetically separated and bent around 1 km arcs, then brought into collisions after being focused to an rms radius of about 3  $\mu\text{m}$ , and finally extracted to dumps.

Typical luminosities are  $3 \times 10^{27} \text{ cm}^{-2} \text{ s}^{-1}$  and the energy spread ( $\sigma_E$ ) of each beam is about  $\pm 0.3\%$ .

The Mark II drift chamber and the calorimeters provide the principal information used in this analysis to identify  $Z$  decays.<sup>2</sup> Charged particles are detected and momentum analyzed in a 72-layer cylindrical drift chamber immersed in a 4.75-kG solenoidal magnetic field. The drift chamber tracks charged particles with  $|\cos\theta| < 0.92$ , where  $\theta$  is the angle to the incident beams. Photons are detected in electromagnetic calorimeters that cover the region  $|\cos\theta| < 0.96$ . The calorimeters in the central region (barrel calorimeters) are lead-liquid-argon ionization chambers, while the end-cap calorimeters are lead-proportional-tube sandwiches.

The detectors for the small-angle  $e^+e^-$  (Bhabha) events used to measure the integrated luminosity are the small-angle monitors (SAM's), which cover the angular region of  $50 < \theta < 165$  mrad. Each SAM consists of nine layers of drift tubes for tracking (not used in this analysis) and a six-layer lead-proportional-tube sandwich for measuring the electron energy and position.

A precise, absolute measurement of the energy of each beam is accomplished by energy spectrometers placed in the extraction lines to the dumps.<sup>3</sup> These spectrometers use the novel technique of measuring the magnetic deflection of each beam by detecting narrow swaths of synchrotron light emitted before and after the beams pass through precision spectrometer magnets. On each pulse the absolute mean center-of-mass energy is determined to better than 40 MeV, and the rms center-of-mass energy spread  $\sigma_E$  is determined to approximately 30% of itself.<sup>4</sup>

The Mark II data-acquisition system contains two redundant triggers for  $Z$  decays. The first, a charged-particle trigger using a fast track-finding processor, requires two or more charged tracks with transverse momenta greater than about 150 MeV/c and  $|\cos\theta| < 0.75$ . The second, a neutral-energy trigger, fires on a single shower depositing at least 3.3 GeV in the barrel calorimeter or 2.2 GeV in an end-cap calorimeter. Monte Carlo (MC) simulations indicate that 99.8% of hadronic  $Z$  decays will satisfy at least one of the triggers.<sup>5</sup> Of the 94 hadronic events in our data sample, 91 satisfied both triggers. A deposition of 6 GeV or more in each SAM also satisfies the data-acquisition trigger.

In the standard model, approximately 70% of  $Z$  decays go into hadrons, 10% into charged-lepton pairs, and 20% into neutrino pairs. We require candidates for  $Z$  hadronic decays to have at least three charged tracks with transverse momentum greater than 110 MeV/c emerge at  $|\cos\theta| < 0.92$  from a cylindrical volume of radius 1 cm and half-length 3 cm parallel to the beam line. To suppress possible contamination from beam-gas or two-photon-exchange interactions, we also require the energy visible in the forward ( $E_f$ ) and backward ( $E_b$ ) hemispheres to be greater than  $0.05E$ . Figure 1 shows

$E_b$  vs  $E_f$  for events satisfying the cut on charged tracks. A MC simulation indicates that we expect 0.005 events in our data from two-photon-exchange interactions. The number of beam-gas interactions that satisfy these cuts is expected to be  $< 0.6$  at the 90% confidence level (C.L.) since no events were found in cylindrical volumes of radius 1 cm and half-length 3 cm displaced  $\pm 10$  and  $\pm 16$  cm from the interaction point. The efficiency for  $Z$  hadronic decays to satisfy these selection requirements, including trigger, is found by a MC simulation to be  $\epsilon_h = (93.7 \pm 0.4)\%$ . The uncertainty is found by varying in the detector simulation the calorimeter energy scales by  $\pm 10\%$  and the tracking efficiency for  $|\cos\theta| > 0.85$  by  $\pm 20\%$ . Backgrounds from the beam are included in the MC detector simulation by combining data from random beam crossings with MC events. They are found to have little effect on the analysis.

We have also included in our fiducial sample  $\mu$  and  $\tau$  pairs with  $|\cos\theta| < 0.65$ , where  $\theta$  is the thrust angle. In this angular region, the trigger efficiency for leptonic events is high and the identification is unambiguous.  $\tau$  events are required to have visible energy greater than  $0.1E$ . The efficiencies for events in this fiducial angular region are found by a MC simulation to be  $\epsilon_\mu = (99 \pm 1)\%$  and  $\epsilon_\tau = (96 \pm 1)\%$ .

Bhabha scattering events in the SAM calorimeters are unmistakable and background free. They follow the expected distributions in polar scattering angle, azimuth, and acollinearity. The resolution in  $\theta$  from reconstructed showers in the SAM calorimeters is 1 mrad except at the edges of the calorimeters. To minimize the systematic error of geometric acceptance cuts while retaining as much statistical power as possible, two overlapping classes of Bhabha events are defined. All 234 events in which at least 40% of the beam energy is detected in each SAM are used for calculating the relative luminosity between scan points. The cross section for these

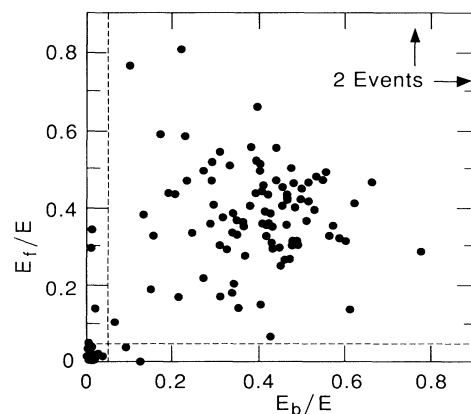


FIG. 1. Forward-hemisphere energy ( $E_f$ ) vs backward-hemisphere energy ( $E_b$ ) for all events satisfying cuts on charged tracks. A MC simulation predicts that four hadronic  $Z$  events should fail the cut in one hemisphere only; we observe six such events.

events is derived by scaling to 143.5 events which fall into a smaller fiducial volume that has an accurately calculable acceptance. These "precise" Bhabha events are those in which  $65 < \theta < 160$  mrad for both  $e^-$  and  $e^+$  showers, plus, with a weight of 0.5, events where one shower is within the precise region and the other shower has  $60 < \theta < 65$  mrad. This weighting reduces the effects of misalignments and detector resolution. The cross section with this precise angular definition is  $24.9 \times [91.1/E \text{ (GeV)}]^2 \text{ nb}$ ,<sup>6</sup> including a +1.5% correction from detector resolution effects. Inefficiencies are negligible. The estimated systematic errors are 2% from unknown higher-order radiative corrections and 2% due to detector resolution effects. Scaling then to the full sample gives a SAM Bhabha cross section of  $\sigma_S = 40.6 \times [91.1/E \text{ (GeV)}]^2 \text{ nb}$ , with an additional 5.3% statistical error due to the scaling factor. We also correct  $\sigma_S$  for the effect of  $Z$ -photon interference which, although small (1%), varies rapidly with  $E$  for  $E \approx M_Z$ .

Table I gives for each scan point the number of  $Z$  hadronic and leptonic decays detected within the fiducial requirements, the number of SAM Bhabha events, and  $\sigma_Z$ .<sup>7</sup> Also listed are the mean energy of the Bhabha events, as measured by the energy spectrometer, and the average  $\sigma_E$  generated by the energy spread of the beams and by the pulse-to-pulse jitter and drifts of the beam energies. The cross sections contain a correction for the energy spread. This correction varies from +3% near the peak to -3% in the tails. In Table I, the ratio of leptonic to hadronic events is  $12/94 = 0.128 \pm 0.053$ . The standard model predicts 0.055 for our fiducial region and efficiencies. There are four  $\mu^+\mu^-$  and eight  $\tau^+\tau^-$  events.

The visible  $Z$  cross section ( $\sigma_Z$ ) can be represented by a relativistic Breit-Wigner resonance shape:

$$\sigma_Z(E) = \frac{12\pi}{m_Z^2} \frac{s\Gamma_e\Gamma_f}{(s - m_Z^2)^2 + s^2\Gamma^2/m_Z^2} [1 + \delta(E)], \quad (1)$$

where  $s \equiv E^2$  and  $\delta$  is the substantial correction due to initial-state radiation calculated using the analytic form given by Cahn.<sup>8</sup> The  $Z$  partial widths into electron pairs and into decays in our fiducial volume are  $\Gamma_e$  and  $\Gamma_f$ , respectively. The partial widths into hadrons, muons,

TABLE I. Number of events, average  $E$  and  $\sigma_E$ , and cross sections for the production of hadronic events and muon and  $\tau$  pairs with  $|\cos\theta| < 0.65$  at each energy setting.

$\langle E \rangle$ (GeV)	$\langle \sigma_E \rangle$ (GeV)	SAM $e^+e^-$	Z decays			$\sigma_Z$ (nb)
			Had.	Lep.	Tot.	
89.24	0.22	24	3	0	3	$5.5 \pm 0.1$
89.98	0.25	37	8	2	10	$11.8 \pm 0.1$
90.70	0.28	44	27	3	30	$30.4 \pm 0.1$
91.50	0.29	53	32	6	38	$31.9 \pm 0.4$
92.16	0.28	33	11	0	11	$14.2 \pm 0.8$
92.96	0.23	43	13	1	14	$13.5 \pm 0.6$
Totals		234	94	12	106	

and  $\tau$  are related to  $\Gamma_f$  by  $\Gamma_f = \Gamma_h + f(\Gamma_\mu + \Gamma_\tau)$ , where  $f = 0.556$  is the fraction of all muon and  $\tau$  decays that have  $|\cos\theta| < 0.65$ . We take the total  $Z$  width to be  $\Gamma = \Gamma_h + \Gamma_e + \Gamma_\mu + \Gamma_\tau + N_\nu\Gamma_\nu$ , where  $N_\nu$  is the number of species of neutrinos.

We estimate  $Z$  resonance parameters by constructing a likelihood function from the probability of observing, at each energy,  $n_Z$   $Z$  decays and  $n_S$  Bhabha scatters given that we have observed a total of  $n_Z + n_S$  events. After eliminating terms that are constant with respect to the fit parameters we obtain for the likelihood  $L$

$$L = \prod \frac{(\epsilon\sigma_Z)^{n_Z}}{(\epsilon\sigma_Z + \sigma_S)^{n_Z + n_S}}. \quad (2)$$

The product is over energy bins and  $\epsilon = 0.941$ . We take the C.L. corresponding to  $n$  standard deviations to be the point at which  $\ln L$  decreases by  $n^2/2$  from its maximum value.

We have performed three fits to the data, which differ in their reliance on the minimal standard model. The first leaves only  $m_Z$  as a free parameter. The widths are those expected for  $Z$  couplings to the known fermions (five quarks and three lepton doublets),<sup>9</sup> including a QCD correction to the hadronic width of 5%. For  $m_Z = 91.11 \text{ GeV}/c^2$  and  $\sin^2\theta_W = 0.2312$ ,  $\Gamma_e = \Gamma_\mu = \Gamma_\tau = 0.083 \text{ GeV}$ ,  $\Gamma_\nu = 0.165 \text{ GeV}$ , and  $\Gamma_h = 1.73 \text{ GeV}$ . The second fit leaves both  $m_Z$  and  $N_\nu$  as free parameters but fixes  $\Gamma_\nu$  and all other partial widths to their expected values. Finally, the third fit leaves  $m_Z$ ,  $N_\nu$ , and  $\Gamma$  free but fixes  $\Gamma_e$ ,  $\Gamma_\mu$ ,  $\Gamma_\tau$ , and  $\Gamma_\nu$  to their expected values. For all fits,  $N_\nu$  depends on the assumed values of  $\Gamma_e$  and  $\epsilon$  and the absolute normalization of  $\sigma_S$ , while  $m_Z$  and  $\Gamma$  are not sensitive to them.

The results of these fits are displayed in Fig. 2 and Table II. Taking the most conservative limit from Table II, we conclude that  $m_Z = 91.11 \pm 0.23 \text{ GeV}/c^2$ . The most important systematic error for the mass determination is the  $\leq 40 \text{ MeV}/c^2$  uncertainty in the absolute energy scale, which is negligible compared to the statistical error. The error on the mass from the third fit is smaller due to the narrower fit width.

The electroweak mixing angle  $\theta_W$ , defined by  $\sin^2\theta_W \equiv 1 - m_W^2/m_Z^2$ ,<sup>10</sup> is related to  $m_Z$  by

$$\sin^2\theta_W = \left[ \frac{4\pi\alpha}{\sqrt{2}G_F m_Z^2 (1 - \Delta r)} \right]^{1/2}. \quad (3)$$

The effects of radiative corrections are represented by

TABLE II.  $Z$  resonance parameters. The three fits are described in the text.

Fit	$m_Z$ (GeV/ $c^2$ )	$N_\nu$	$\Gamma$ (GeV/ $c^2$ )	$\chi^2/N_{DF}$
1	$91.11 \pm 0.23$	...	...	4.1/5
2	$91.11 \pm 0.23$	$3.8 \pm 1.4$	...	3.7/4
3	$91.06 \pm 0.17$	$3.2 \pm 1.3$	$1.61 \pm 0.40$	1.5/3

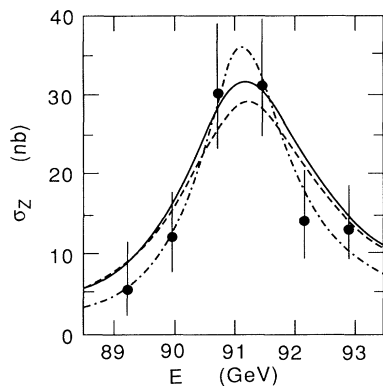


FIG. 2.  $e^+e^-$  annihilation cross sections to all hadronic events plus  $\mu$  and  $\tau$  pairs with  $|\cos\theta| < 0.65$ . The curves represent the result of different fits: solid,  $m_Z$  free; dashed,  $m_Z$  and  $N_\nu$  free; and dot-dashed,  $m_Z$ ,  $N_\nu$ , and  $\Gamma$  free. The peak  $\sigma_Z$  occurs approximately 100 MeV higher than  $m_Z$  due to radiative corrections.

$\Delta r$ .<sup>11</sup> With  $m_Z = 91.11 \pm 0.23$  GeV/ $c^2$ ,  $\sin^2\theta_W = 0.2312 \pm 0.0017$  for a top mass ( $m_t$ ) of 100 GeV/ $c^2$  and a Higgs-boson mass ( $m_H$ ) of 100 GeV/ $c^2$ . The dependence of  $\sin^2\theta_W$  on  $m_t$  and  $m_H$  is shown in Fig. 3.

Previous direct measurements of  $m_Z$  by  $p\bar{p}$  colliders yielded  $93.1 \pm 1.0 \pm 3.1$  GeV/ $c^2$  (UA1)<sup>12</sup> and  $91.5 \pm 1.2 \pm 1.7$  GeV/ $c^2$  (UA2),<sup>13</sup> where the first error is statistical and the second reflects the uncertainty in the overall mass scale.

The third fit yields  $\Gamma = 1.61^{+0.60}_{-0.43}$  GeV, which should be compared to the standard-model value of 2.48 GeV. The systematic error on this value is 30 MeV due to uncertainty in the relative energy of scan points. If we assume that  $\Gamma$  can only be larger than this value, then at the 90% C.L.,  $\Gamma < 3.1$  GeV. Previous direct measurements of  $\Gamma$  yielded upper limits at the 90% C.L. of 5.2 GeV (UA1)<sup>12</sup> and 5.6 GeV (UA2).<sup>13</sup>

We use the second fit for  $N_\nu$ ,  $N_\nu = 3.8 \pm 1.4$ , corresponding to a partial width to invisible decay modes of  $N_\nu\Gamma_\nu = 0.62 \pm 0.23$  GeV. At the 90% C.L.,  $N_\nu < 5.5$ . The 6.1% uncertainty in  $\sigma_S$  contributes  $\pm 0.6$  to the error. Previous measurements of  $N_\nu$  by detection of single photons in  $e^+e^-$  annihilation gives  $N_\nu < 5.2$ .<sup>14</sup> The third-fit result for  $N_\nu$  assumes standard-model values of  $\Gamma_e$  and  $\Gamma_\nu$ , an assumption that may be incompatible with a measurement of  $\Gamma$  less than the standard model.

We express our profound appreciation to the SLAC staff for the dedicated and monumental effort of bringing the technology of linear  $e^+e^-$  colliders to fruition. We also thank Robert Cahn, Bryan Lynn, and Michael Peskin for assistance with the interpretation of the measurements. This work was supported in part by the Department of Energy Contracts No. DE-AC03-81ER40050 (California Institute of Technology), No. DE-AM03-76SF00010 (University of California, Santa Cruz), No. DE-AC02-86ER40253 (University of Colorado), No. DE-AC03-83ER40103 (University of Hawaii), No. DE-AC02-84ER40125 (Indiana University), No. DE-

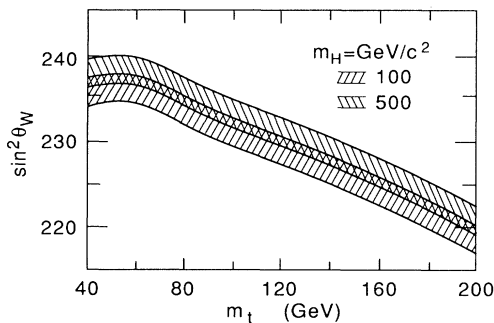


FIG. 3. Value of  $\sin^2\theta_W$  as a function of the top mass, for Higgs-boson masses of 100 and 500 GeV/ $c^2$ . The width of each band represents the uncertainty in  $\sin^2\theta_W$  corresponding to the uncertainty in  $m_Z$ .

AC03-76SF00098 (LBL), No. DE-AC02-76ER01112 (University of Michigan), and No. DE-AC03-76SF-00515 (SLAC), and by the National Science Foundation (Johns Hopkins University).

<sup>1</sup>B. Richter, SLAC Report No. SLAC-229, 1980 (unpublished); D. L. Burke, SLAC Report No. SLAC-PUB-4851, 1989 (to be published).

<sup>2</sup>G. Abrams *et al.*, SLAC Report No. SLAC-PUB-4558, 1989 [Nucl. Instrum. Methods (to be published), and references therein].

<sup>3</sup>J. Kent *et al.*, SLAC Report No. SLAC-PUB-4922, 1989 (to be published); M. Levi, J. Nash, and S. Watson, SLAC Report No. SLAC-PUB-4654 [Nucl. Instrum. Methods (to be published)]; M. Levi *et al.*, SLAC Report No. SLAC-PUB-4921, 1989 (to be published).

<sup>4</sup>There were a few events for which one of the spectrometer energies was not available. In these cases, the missing-energy measurement was supplied by an auxiliary system which had been calibrated to the energy spectrometer.

<sup>5</sup>The first energy-scan point at 92.2 GeV had a somewhat more restrictive trigger which lowered the efficiency by 1.1%.

<sup>6</sup>F. A. Berends, R. Kleiss, and W. Hollik, Nucl. Phys. **B304**, 712 (1988); S. Jadach and B. F. L. Ward, University of Tennessee Report. No. UTHEP-88-11-01, 1988 (to be published).

<sup>7</sup>The errors listed are 68.3%-C.L. intervals. F. James and M. Roos, Nucl. Phys. **B172**, 475 (1980).

<sup>8</sup>R. N. Cahn, Phys. Rev. D **36**, 2666 (1987), Eqs. (4.4) and (3.1). See J. Alexander *et al.*, Phys. Rev. D **37**, 56 (1988) for a comparison of different radiative correction calculations.

<sup>9</sup>Weak radiative corrections are small when widths are calculated using  $G_F$ . W. F. L. Hollik, DESY Report No. DESY 88-188, 1988 (to be published). Note that widths in Table 5.1 of this paper do not include QCD corrections.

<sup>10</sup>A. Sirlin, Phys. Rev. D **22**, 971 (1980).

<sup>11</sup>W. J. Marciano and A. Sirlin, Phys. Rev. D **22**, 2695 (1980).

<sup>12</sup>C. Albajar *et al.*, CERN Report No. CERN-EP/88-168, 1988 (to be published).

<sup>13</sup>R. Ansari *et al.*, Phys. Lett. B **186**, 440 (1987).

<sup>14</sup>The combined ASP, MAC, and CELLO result is calculated in C. Hearty *et al.*, Phys. Rev. D **39**, 3207 (1989).